JOURNAL OF GEOPHYSICAL RESEARCH, VOL. 89, NO. A10, PAGES 8971–8985, OCTOBER 1, 1984

Correlated Low-Frequency Electric and Magnetic Noise Along the Auroral Field Lines

D. A. GURNETT AND R. L. HUFF

Department of Physics and Astronomy, University of Iowa, Iowa City

J. D. MENIETTI, J. L. BURCH, AND J. D. WINNINGHAM

Southwest Research Institute, San Antonio, Texas

S. D. SHAWHAN

NASA Headquarters, Washington, D. C.

Plasma wave and plasma measurements from the Dynamics Explorer 1 (DE 1) spacecraft are used to investigate an intense broadband spectrum of low-frequency, <100 Hz, electric and magnetic noise observed at low altitudes over the auroral zones. This noise is detected by DE 1 on essentially every low-altitude pass over the auroral zone and occurs in regions of low-energy, 100 ev to 10 keV, auroral electron precipitation and field-aligned currents. The electric field is randomly polarized in a plane perpendicular to the static magnetic field. Correlation measurements between the electric and magnetic fields show that the perpendicular ($\sim$north-south) electric field fluctuations are closely correlated with the perpendicular (east-west) magnetic field fluctuations and that the Poynting flux is directed downward, toward the earth. The total electromagnetic power flow associated with the fluctuations is large, approximately 10^8 W. Two general interpretations of the low-frequency noise are considered: first, that the noise is produced by static fields imbedded in the ionosphere and, second, that the noise is due to Alfven waves propagating along the auroral field lines. For the static interpretation the ratio of the magnetic to electric field strengths at the base of the ionosphere is determined by the Pedersen conductivity, $B/(\mu_0 E) = \Sigma_P$, whereas for the Alfven wave interpretation it is determined by the Alfven index of refraction, $cB/E = n_A$. Measurements show that the magnetic to electric field ratio decreases rapidly with increasing height. This height dependence is in strong disagreement with the static model if the magnetic field lines are assumed to be equipotentials ($E_{\parallel} = 0$). At present, no satisfactory model is available for comparison with the data if an electrostatic potential drop is assumed to exist along the magnetic field ($E_{\parallel} \neq 0$). The Alfven wave model is in good agreement with the general form of the height dependence of the magnetic to electric field ratio but disagrees in certain details. The cB/E ratio tends to decrease with increasing frequency and is usually somewhat larger than the computed value of the Alfven index of refraction. Some of these difficulties could be accounted for by reflections at the base of the ionosphere or propagation at large angles to the magnetic field (kinetic Alfven waves). For both the static model and the Alfven wave model the source must be located at high altitudes, since the average Poynting flux is always directed downward, even at radial distances up to 2 R_E.

1. INTRODUCTION

One of the most prominent and commonly occurring types of noise detected by the plasma wave instrument on the Dynamics Explorer 1 (DE 1) spacecraft is an intense, broadband, $f \lesssim 100$ Hz, spectrum of electric and magnetic noise at low altitudes over the auroral zones. The DE 1 observations of this noise are not new. The existence of intense low-frequency electric field noise at altitudes of a few thousand kilometers over the auroral zones was first reported by *Heppner* [1969] using electric field measurements from the OV1-10 spacecraft. This noise was subsequently described and studied by a number of investigators, including *Maynard and Heppner* [1970], *Kelley and Mozer* [1972], *Kintner* [1976], *Temerin* [1978], *Maynard et al.* [1982], and *Curtis et al.* [1982]. Typically, the noise occurs over a frequency range from a few hertz to several hundred hertz, decreasing in intensity with increasing frequency. Somewhat similar broadband electric field noise was also reported by *Gurnett and Frank* [1977] along the auroral field lines at altitudes of several earth radii and higher. However, because of the markedly different plasma parameters at these higher altitudes, it has never been clear that the broadband electrostatic noise observed at high altitudes is the same as the noise observed at lower altitudes.

It is widely believed that the low-altitude electric field noise is caused by the motion of the spacecraft through static electric field structures in the ionosphere. The frequency detected by the spacecraft is then entirely determined by the Doppler shift. This interpretation was first proposed by *Heppner* [1969] and has been given strong support by *Temerin* [1978], who showed that short-wavelength antenna interference effects are present in the spectrum of the low-frequency noise. These interference effects demonstrate that in some cases the wavelengths of the noise can be very short; only a few tens of meters or less. Wavelengths in this range produce Doppler shifts of several hundred hertz or more at typical spacecraft velocities.

Irregular magnetic field fluctuations are also a common feature of low-altitude satellite magnetic field measurements in the auroral zone [*Zmuda and Armstrong*, 1974*a*, *b*]. At low frequencies, below a few tens of hertz, these magnetic field fluctuations are usually interpreted as being due to the motion of the spacecraft through a system of static field-aligned currents linking the auroral zone and the distant magnetosphere.

Paper number 4A0856.
0148-0227/84/004A-0856$05.00

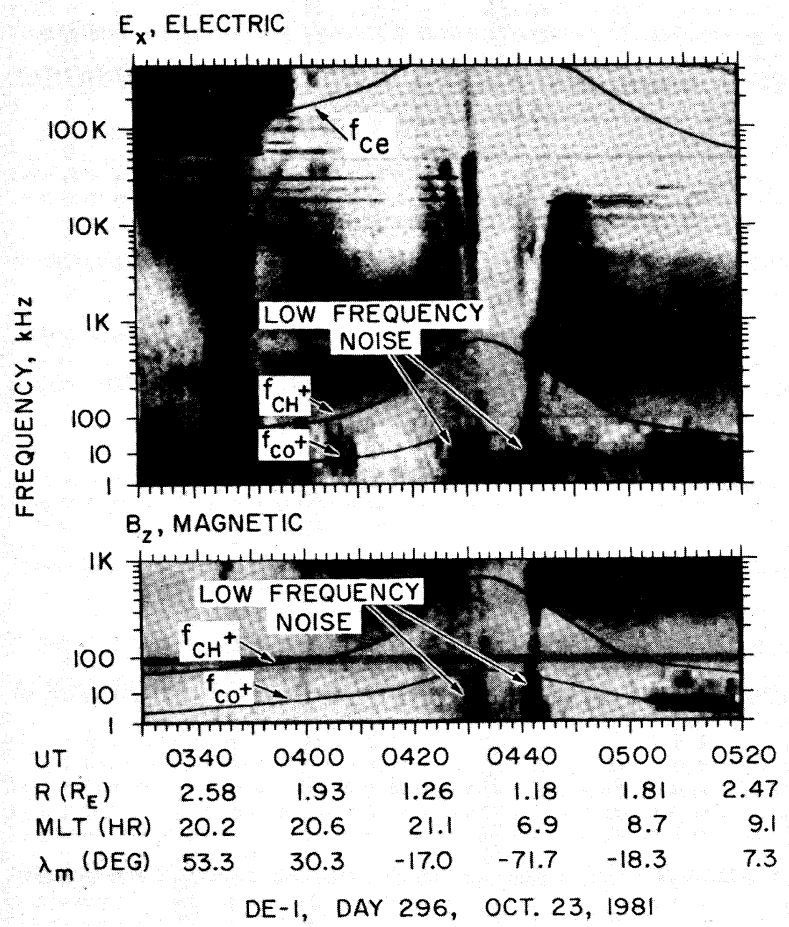

Fig. 1. Typical DE-1 electric and magnetic field spectrograms showing the low-frequency electric and magnetic field noise observed at low altitudes over the auroral zones. Note that the low-frequency noise occurs over both the evening and morning auroral regions but is almost completely absent over the polar cap.

For a recent review of field-aligned currents in the auroral regions, see *Potemra* [1983]. Using data from the Hawkeye 1 spacecraft, *Kintner* [1976] showed that the electric field noise and the magnetic field noise occur in the same region and that both types of noise have similar spectrums, varying approximately as $f^{-2.8}$ for the electric field and as $f^{-4.0}$ for the magnetic field. The noise also occurs in regions with large shears in the east-west convection velocity. These observations led Kintner to suggest that the noise is two-dimensional magnetohydrodynamic (MHD) turbulence excited by a shear-driven instability. For a further discussion of two-dimensional MHD turbulence processes in the auroral regions, see *Kelley and Kintner* [1978].

In this paper we describe the DE-1 observations of the low-frequency auroral zone noise and discuss the relationship of these observations to low-energy plasma measurements on the same spacecraft. Compared with previous observations, the DE-1 plasma wave measurements provide a new capability for determining the correlation between various components of the electric and magnetic field, thereby giving new information on the character of the noise. The DE-1 data also provide measurements over a range of altitudes along the auroral field lines that have not been previously surveyed. For a description of the plasma wave instrument on DE-1, see *Shawhan et al.* [1981], and for a description of the plasma instrument, see *Burch et al.* [1981].

2. Basic Characteristics and Region of Occurrence

To illustrate the general characteristics of the low-frequency electric and magnetic field noise, we will now describe some representative events and discuss the region of occurrence of the noise. A typical example is shown in Figure 1. The top panel of this illustration shows a frequency-time spectrogram of the electric field detected by DE-1 during a low-altitude pass over the southern polar region on October 23, 1981. The bottom panel shows the corresponding magnetic field spectrogram. To interpret these spectrograms, it is necessary to understand the geometry of the orbit. DE-1 is in a highly eccentric polar orbit with an apogee geocentric radial distance of 4.65 R_E and a perigee geocentric radial distance of 1.1 R_E. At the time of the pass shown in Figure 1 the perigee was located over the southern polar region. Because of the high spacecraft velocity near perigee, the spacecraft passes over the southern polar region very quickly. The spacecraft crosses through the evening auroral zone from about 0428 to 0433 UT, passes over the polar cap from about 0433 to 0440 UT, and crosses through the morning auroral zone from about 0440 to 0444 UT. The dark portions of the spectrogram indicate regions of higher intensity. The low-frequency electric and magnetic field noise is clearly evident over the evening and morning auroral zones at frequencies extending up to about 50 Hz.

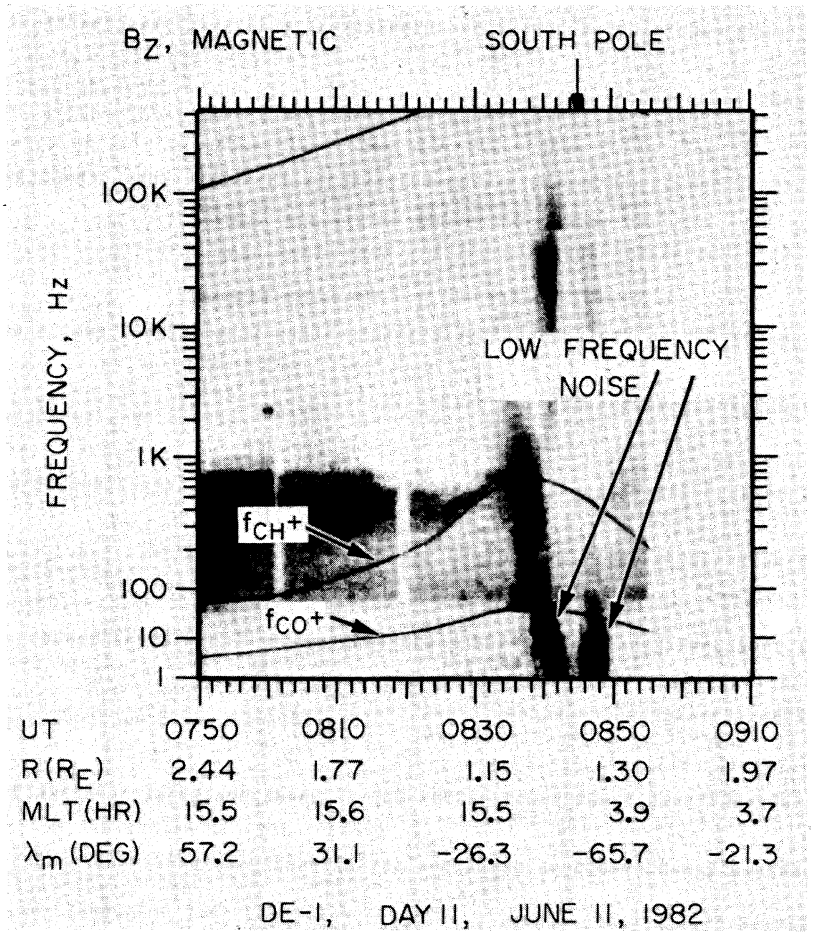

Fig. 2. Another example of the low-frequency electric and mangetic field noise during a pass about 3 months after the event in Figure 1. Very similar low-frequency noise spectrums are observed on essentially all low-altitude passes over the auroral zones.

Usually, the low-frequency electric and magnetic field noise is most intense in the lowest, 1.78 Hz, frequency channel and decreases in intensity with increasing frequency. For reference the cyclotron frequencies for protons, f_{cH^+}, and singly charged oxygen, f_{cO^+}, are shown in Figure 1. As can be seen, most of the energy in the spectrum is concentrated below the O^+ cyclotron frequency. Although the noise sometimes appears to have a cutoff near the O^+ cyclotron frequency, cases can also be found where the spectrum extends well above f_{cO^+}, particularly for the electric field. For example, during the morning auroral zone crossing in Figure 1, 0440 to 0444 UT, the electric field spectrum can be seen extending well above the O^+ cyclotron frequency. In some of these cases the high-frequency electric field noise appears to be of entirely different origin, either auroral hiss, or ELF noise bands of the type reported by *Gurnett and Frank* [1972] and *Temerin and Lysak* [1984]. With the available frequency resolution it is often difficult to determine the transition between these different types of noises.

Another example of the low-frequency electric and magnetic noise is shown in Figure 2. This illustration shows a magnetic field spectrogram from a pass over the southern polar cap on January 11, 1982, about 3 months after the pass in Figure 1. The low-frequency noise is again clearly evident over the two auroral zones, from 0838 to 0843 UT in the local evening and from 0846 to 0849 UT in the local morning. The tendency for most of the energy to be concentrated below the O^+ cyclotron frequency is again evident. Examination of all the passes that occurred during this period shows that the low-frequency noise persists with very similar characteristics from one orbit to the next over a period of at least several months. The width of the region of enhanced noise levels and the peak intensities vary somewhat from orbit to orbit, but the noise is essentially always detectable.

To determine the region of occurrence of the low-frequency noise, a survey was performed of all the available DE 1 spectrograms obtained over a 2-year period, from September 1981 to September 1983. Events were selected by requiring that a broadband enhancement be evident simultaneously on both the electric and magnetic spectrograms at frequencies below the O^+ cyclotron frequency. The thresholds for identifying the noise on the spectrograms correspond to electric and magnetic spectral densities at 10 Hz of about 2×10^{-14} V^2 m^{-2} Hz^{-1} and 1×10^{-6} nT^2 Hz^{-1}. Using this criterion, a total of 87 events were identified. Figure 3 shows the spacecraft trajectory for all of the events identified plotted as a function of radial distance and magnetic latitude. It is evident that the noise occurs at all altitudes along the auroral field lines up to radial distances of at least 2 R_E. Usually, the intensity and upper frequency limit of the magnetic noise decrease with increasing altitude. The electric field spectrum is more complicated and tends to spread upward in frequency with increasing altitude,

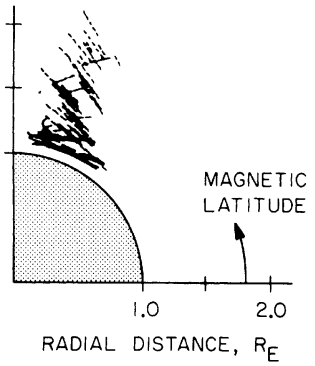

Fig. 3. A magnetic meridian plane plot of all of the low-frequency noise events detected by DE-1 over a 2-year period. The noise occurs continuously along the auroral L shells at radial distances up to about 2 R_E. Note the tendency for the latitudinal width to increase with decreasing altitude.

merging into a broadband spectrum characteristic of the broadband electrostatic noise described by *Gurnett and Frank* [1977]. The region of occurrence in Figure 3 does not extend to the higher altitudes reported by *Gurnett and Frank* [1977] because we demanded the simultaneous presence of both electric and magnetic noise. Since the broadband electrostatic noise is quite common at higher altitudes, the upper altitude cutoff of the events in Figure 3 is mainly determined by the magnetic noise.

The distribution of the low-frequency noise in magnetic local time and invariant latitude is shown in Figure 4. Except for gaps in the early morning and early afternoon, the noise occurs at essentially all local times. The gaps in the early morning and early afternoon are believed to be a sampling effect caused by secular changes in the orbit. Because of the combined effect of the latitudinal motion of perigee and the change in the local time of the orbit plane, no low-altitude passes are available in the present data set in the early morning and early afternoon.

3. Relationship to Auroral Precipitation

To investigate the relationship between the low-frequency electric and magnetic noise and the auroral zone, we have studied the DE 1 plasma measurements for a number of the events described in the preceding section. A typical example is shown in Figure 5. The top panel of this illustration shows the magnetic field spectrogram for a low-altitude pass over the southern polar region on October 25, 1981, 2 days after the event shown in Figure 1. As usual the low-frequency noise can be identified over the two auroral zone crossings, from 0425 to 0428 UT in the local evening and from 0434 to 0439 UT in the local morning. For comparison the low-energy electron flux, electron density, and field-aligned current density are shown in the bottom three panels, which are expanded to cover the time interval from 0424 to 0442 UT. These parameters were obtained by integrating over electron energies from 56 to 13,206 eV. The regions of intense low-frequency noise are indicated by shading. Well-defined ehancements of the electron flux and electron density are evident in the region where the noise is observed. The low-energy electron fluxes, $\sim 10^9$ to 10^{10} cm^{-2} s^{-1}, and electron densities, $\sim 10^{-1}$ to 1.0 cm^{-3}, are typical of the electron precipitation commonly observed in the auroral regions. Usually, little or no proton precipitation is observed in these regions. The bottom panel of Figure 5 shows that the low-frequency noise is also closely associated with regions of enhanced field-aligned current densities. The current densities are computed from the measured electron distribution function, integrated over the energy range, 56 to 13,206 eV. Most of the contribution to the field-aligned current comes from low-energy electrons with energies of a few hundred eV.

Another example comparing the low-frequency electric and magnetic field noise and the low-energy electron measurements is shown in Figure 6. This example is for the pass over the southern polar region shown in Figure 1, on October 23, 1981. The top panel of Figure 6 shows the magnetic field spectral density on an expanded time scale, and the bottom three panels show the electron flux, electron density, and field-aligned current density. The regions of intense low-frequency noise are indicated by shading. Again the noise is seen to occur only in regions of enhanced electron flux characteristic of the auroral zone and in regions of enhanced field-aligned current density.

4. Electric and Magnetic Field Spectrums and Correlations

To help determine the type of disturbance responsible for the low-frequency electric and magnetic noise, we have performed a detailed study of the electric and magnetic field spectrums, including the variation with radial distance and the correlation between the various field components. Comparisons of simultaneously measured electric and magnetic field spectrums are shown in Figures 7 and 8. The spectrums in Figure 7 are from the pass on October 23, 1981, shown in Figure 1, and the spectrums in Figure 8 are from the pass on January 11, 1982, shown in Figure 2. The spectrums have been selected from times of maximum intensity during the pass. At low frequencies the spectrums decrease monotonically with increasing frequency. As described by *Kintner* [1976], the electric and magnetic field spectrums can be roughly described by power laws, with indices of about -2.8 and -4.0, respectively. However, substantial deviations from a power law often occur. We find that in the frequency range from 1 to 100 Hz as much as 30% of the time the spectrum has a peak or a change in slope that deviates by more than 1 order of magnitude from a power law. When deviations from a power law occur, the

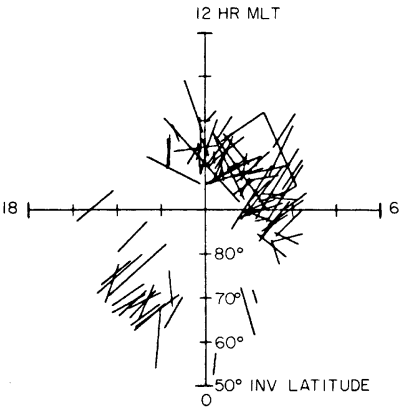

Fig. 4. An invariant latitude/magnetic local time plot of all of the low-frequency noise events detected by DE-1 over a 2-year period. The noise occurs at essentially all local times. The gaps in the early morning and early afternoon are in regions where no low-altitude data are available.

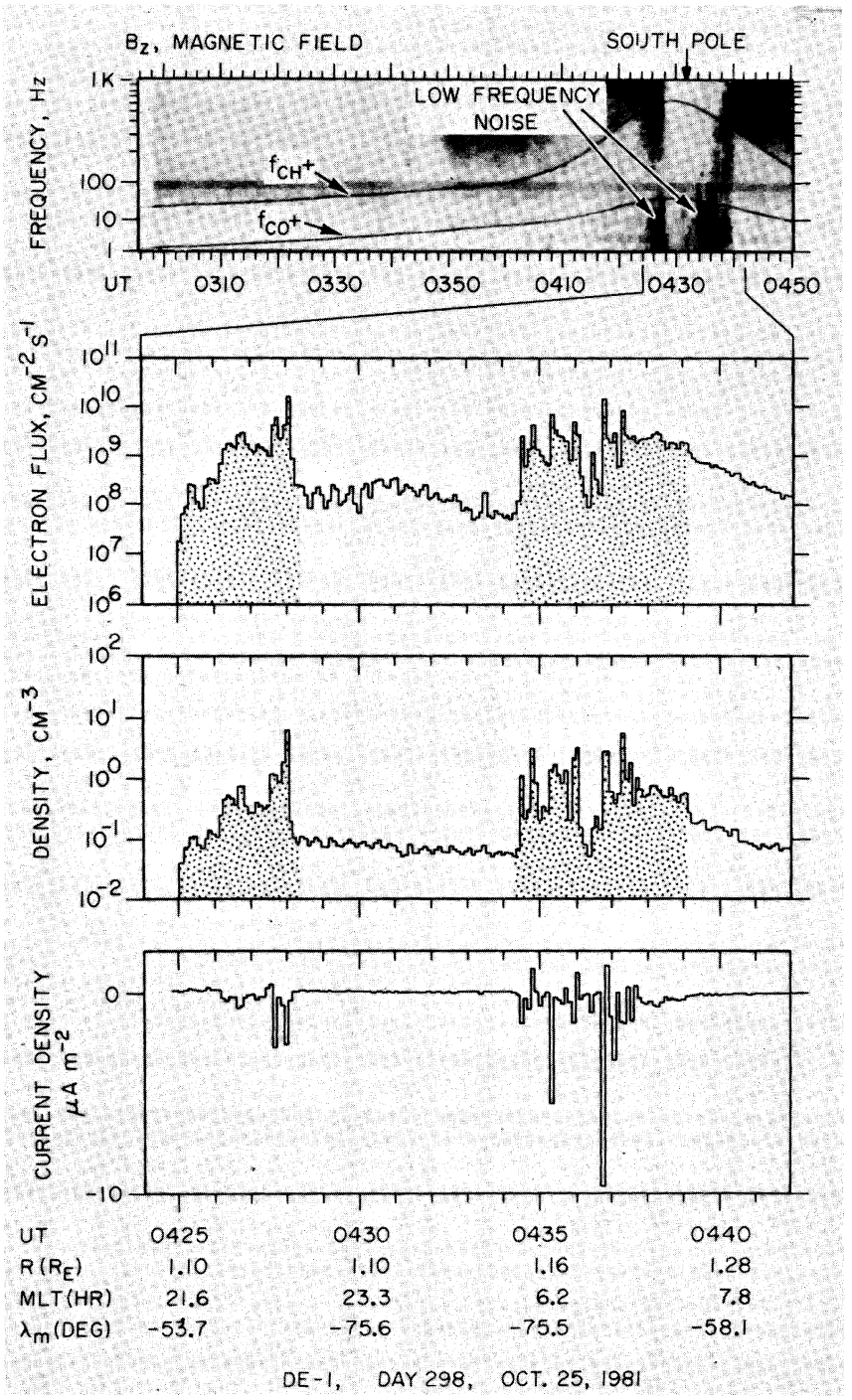

Fig. 5. A comparison of the DE-1 low-energy, 56–13,206 eV, electron measurements with the low-frequency noise observed on a low-altitude pass over the southern polar region on October 25, 1981. The intense low-frequency noise (shaded) occurs in regions of low-energy electron fluxes and field-aligned currents typical of the auroral zone.

electric and magnetic field spectrums tend to have the same shape, particularly at frequencies below a few hundred hertz. If the electric field spectrum has a peak or a change in slope, then this feature is usually also present in the magnetic field spectrum. One is given the strong impression that the electric and magnetic field spectrums are closely related.

Except for various types of electromagnetic emissions at high frequencies, the magnetic field spectral density usually drops below the instrument noise level at frequencies above about 50 Hz. In some cases the magnetic field spectrum shows evidence of a cutoff or change in slope near the O^+ cyclotron frequency, as in Figure 8. Cutoffs in the electric field spectrum at the O^+ cyclotron frequency occur less frequently and are not as convincing as for the magnetic field. Usually, most of the electric field energy is below the O^+ cyclotron frequency, but often a weak component extends across the cyclotron frequency to higher frequencies. Since whistler mode auroral hiss and other types of electrostatic noise are usually present at

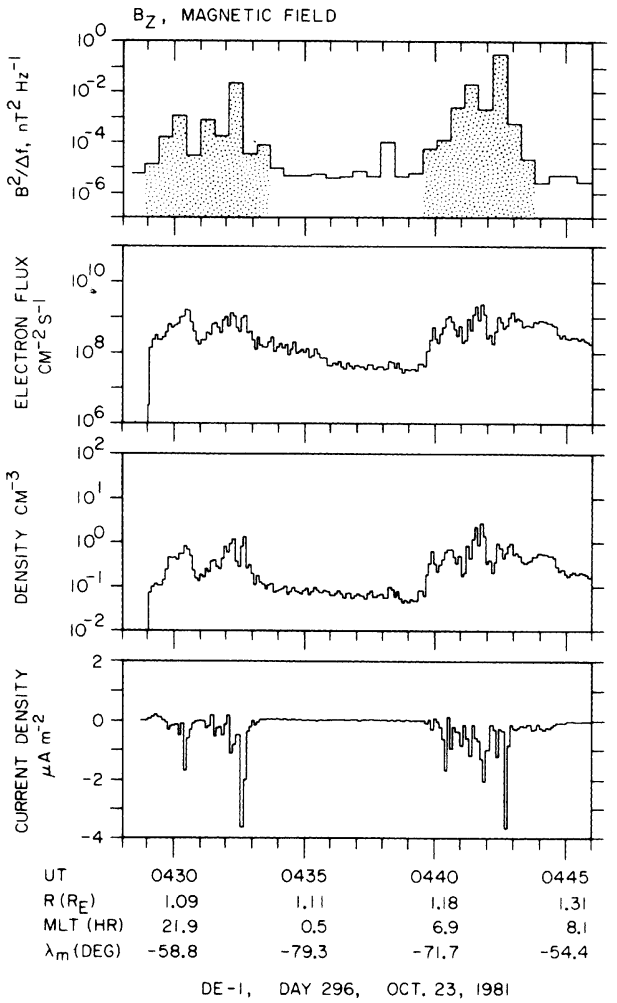

Fig. 6. Another example showing the relationship between the low-frequency magnetic noise, shown in the top panel, and the low-energy electron measurements, shown in the bottom three panels. The low-frequency noise is closely related to the region of field-aligned currents linking the auroral zone and the distant magnetosphere.

higher frequencies, one is left with the strong impression that two different types of noise may be overlapping in this part of the spectrum.

The average electric and magnetic field intensities for all of the events studied are shown in Figure 9 plotted as a function of radial distance. Although the intensities vary considerably from event to event, the average field strengths show a systematic dependence on radial distance. At low frequencies the electric field intensities are nearly independent of altitude, but at high frequencies (>10 Hz) the intensities tend to increase with increasing altitude. At all frequencies the magnetic field intensities decrease with increasing altitude.

To characterize the relationship between the electric and magnetic field spectrum, it is useful to compute the ratio of the magnetic to electric field strength. This ratio is shown as a function of frequency in the top panel of Figures 7 and 8, expressed in terms of an index refraction, $n = cB/E$, on the left, and a conductivity, $\Sigma = B/(\mu_0 E)$, on the right. Possible interpretations of these two quantities are discussed in the next section. The magnetic to electric field ratio is either independent of frequency, as in Figure 7, or decreases slowly with increasing frequency, as in Figure 8. The average values of cB/E and $B/(\mu_0 E)$ for all of the events studied is shown in Figure 10, plotted as a function of radial distance for various frequencies. Although considerable scatter exists in the individual data points, Figure 10 clearly shows that the average magnetic to electric field ratio decreases with increasing altitude. Figure 10 also shows that the magnetic to electric field ratio tends to decrease with increasing frequency, varying approximately as $f^{-0.5}$ at low altitudes and approximately as $f^{-1.0}$ at higher altitudes. The tendency for cB/E to decrease with increasing frequency has been previously noted by *Kintner* [1976]. At low altitudes, $R \simeq 1.1$ to 1.2 R_E, the average magnetic to electric field ratio, cB/E, is usually in the range 200–2000, and the average conductivity, $B/(\mu_0 E)$, is usually in the range 0.5–5.0 mho.

Further information on the relationship between the low-frequency electric and magnetic field noise can be obtained from the correlator incorporated in the DE 1 plasma wave instrument. The correlator gives the correlation coefficient and relative phase between signals received by any selected pair of antennas. An example of the output of the correlator is shown in Figure 11 for a low-frequency noise event observed at low altitudes over the southern auroral zone on September 24, 1981. In this case the correlator was connected to the B_z search coil magnetic antenna and the E_x electric dipole antenna. The B_z antenna is parallel to the spin axis, and the E_x antenna is perpendicular to the spin axis. Since the DE 1 spin axis is perpendicular to the orbital plane, the B_z antenna measures the east-west component of the magnetic field. As the spacecraft rotates, the E_x antenna alternately measures the perpendicular ($\sim$north-south) and parallel ($\sim$field aligned) components of the electric field. The correlation coefficient and relative phase are measured in a narrow frequency band controlled by the stepping of the sweep frequency receiver. During the 32-s interval shown in Figure 11, the correlator steps through four frequency bands, 1.78 Hz, 3.11 Hz, 5.62 Hz, and 10.0 Hz, each with a bandwidth of about $\pm 15\%$. The center frequencies of these bands are indicated at the top of Figure 11. The top two panels show the amplitude of the E_x and B_z fields, and the bottom two panels show the relative phase ϕ and the correlation coefficient ρ between the E_x and B_z fields. The vertical dashed lines indicate times when the $+x$ antenna axis is parallel to the earth's magnetic field, $\mathbf{B}_0$, projected into the spin plane. Because the earth's magnetic field is usually within a few degrees of the spin plane, the E_x antenna axis is very nearly parallel to the earth's magnetic field at these times.

Inspection of Figure 11 shows that the E_x amplitude tends to have a minimum when the $+x$ antenna axis is parallel or antiparallel to the earth's magnetic field. This spin modulation indicates that the electric field is oriented mainly perpendicular to the magnetic field. No spin modulation is evident in the B_z amplitude because this axis is parallel to the spin axis. The bottom panel of Figure 11 shows that the correlation coefficient between the E_x and B_z fields is large, typically greater than 80%. Roughly twice per rotation the correlation coefficient briefly drops to a low value. These minimums in the correlation coefficient occur at minimums in the electric field intensity, when the $+x$ antenna axis is parallel or antiparallel to the earth's magnetic field. The second panel from the bottom shows that the relative phase between the E_x and B_z fields alternates back and forth between $\phi = 0°$ and $\phi = 180°$, producing a clearly defined square wave pattern. The transi-

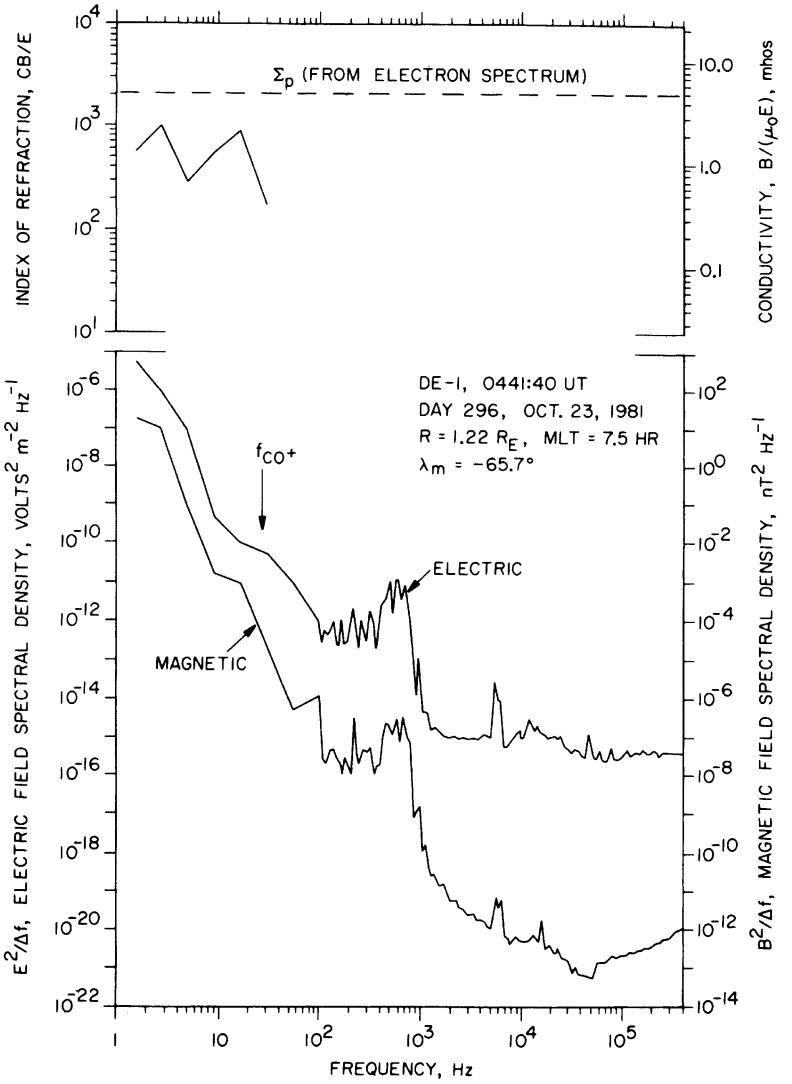

Fig. 7. An example of simultaneously measured electric and magnetic field spectrums for a low-frequency noise event detected by DE-1. Note that most of the energy in the spectrum is concentrated at frequencies below the O^+ cyclotron frequency, f_{cO^+}. The top panel shows the magnetic to electric field ratio in terms of the index of refraction, cB/E, and in conductivity, $B/(\mu_0 E)$.

tions between $\phi = 0°$ and $\phi = 180°$ occur then the $+x$ antenna axis is parallel or antiparallel to the earth's magnetic field. The high correlation coefficient and the square wave phase pattern show that the fluctuations in the perpendicular (east-west) component of the magnetic field and the perpendicular (~north-south) component of the electric field are closely correlated. Careful consideration of the directions involved shows that the fluctuations are such that the Poynting flux, $\mathbf{S} = \mathbf{E} \times \mathbf{B}/\mu_0$, is directed downward along the magnetic field line, toward the earth. Investigation of other similar cases always shows the same basic pattern. Although the correlation coefficient is not always as high as shown in Figure 11, it is usually greater than 50%, and whenever a clearly defined square wave pattern can be seen in the phase plot, the Poynting flux is directed toward the earth. By integrating over typical electric and magnetic field spectrums, as in Figures 7 and 8, and using a representative correlation coefficient, the electromagnetic energy flux associated with the noise can be estimated. Integrated from 1 Hz to 100 Hz, one finds for a typical event that $E_x \simeq 3$ mV m^{-1}, $B_z \simeq 10$ nT, and $\rho \simeq 0.8$, which gives $S \simeq 2 \times 10^{-2}$ erg cm^{-2} s^{-1}. This energy flux is about 0.1 to 1% of the electron energy flux precipitated in the auroral regions.

The polarization of the electric field fluctuations in a plane perpendicular to the magnetic field can also be obtained by selecting times when the E_x and E_z electric antennas are connected to the correlator. An example of an event where the electric field polarization can be measured with this technique is shown in Figure 12. Again, clearly defined minimums can be seen in the E_x field amplitude when the $+x$ antenna axis is parallel or antiparallel to the earth's magnetic field. No spin modulation is evident in the E_z field amplitude because this antenna axis is parallel to the spin axis. The correlation coefficient between the E_x and E_z fields is seen to be relatively high, typically exceeding 50%. However, a consistent square wave spin modulation pattern is not evident in the phase plot. The absence of a spin modulation pattern in the phase plot indicates that even though the fields may be correlated on

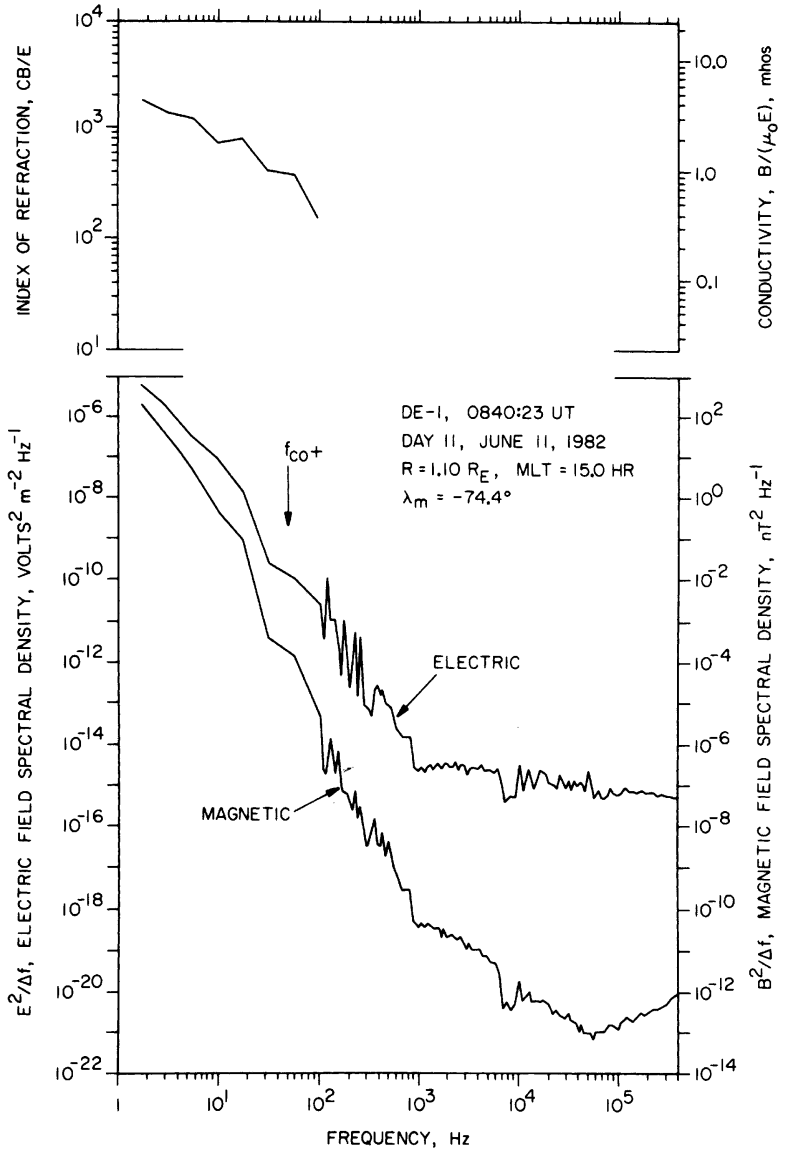

Fig. 8. Another set of spectrums comparable to Figure 7. Note that the magnetic spectrum has a distinct drop in intensity slightly below the O^+ cyclotron frequency, f_{co+}.

short time scales, the polarization is essentially random on a time scale comparable to the spacecraft rotation period. Other cases investigated show the same result. Therefore, it must be concluded that the polarization of the perpendicular component of the electric field is essentially random. No evidence is found for a consistent right- or left-hand polarization with respect to the earth's magnetic field. Polarization measurements could not be performed on the magnetic field because only one magnetic sensor is available for magnetic field measurements.

5. Possible Interpretations

Several interpretations can be advanced to explain the origin of the electric and magnetic noise observed along the auroral field lines. These interpretations can be classified as either a static model or an Alfven wave model. These models can be further subclassified on the basis of whether the electric field component parallel to the static magnetic field is assumed to be zero ($E_{||} = 0$) or nonzero ($E_{||} \neq 0$). We now consider these various interpretations in detail.

5.1. *Static Model ($E_{||} = 0$)*

In the static model the noise is attributed to the motion of the spacecraft through static electric and magnetic field structures in the ionosphere. The frequency spectrum is then determined entirely by the Doppler shift, $\omega = \mathbf{k}\cdot\mathbf{v}$. In this interpretation the possible association of features in the spectrum with the O^+ cyclotron frequency would have to be completely coincidental, because the Doppler shift bears no relationship to the cyclotron frequency. At a typical spacecraft velocity of about 10 km/s a Doppler shift of 50 Hz requires spatial scale lengths of about 200 m. This length scale is small, but not unreasonably small for auroral phenomena. Auroral arcs with thicknesses of only a few hundred meters have been reported [*Akasofu*, 1965].

Because of the high conductivity along the magnetic field

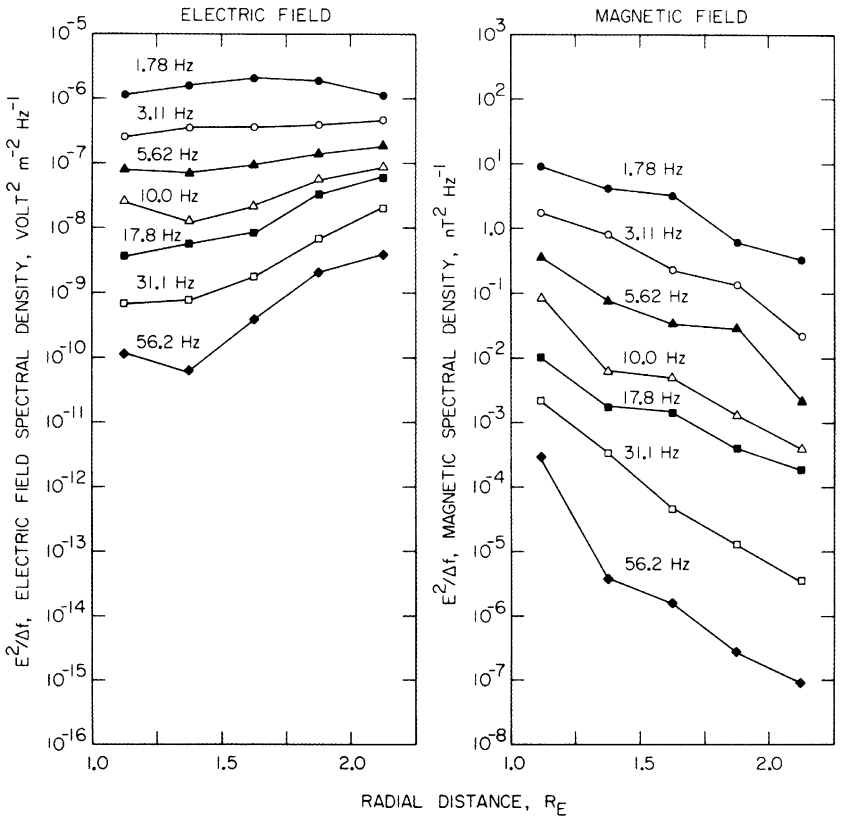

Fig. 9. Plots showing the variation of the average electric the magnetic field intensities with radial distance from the earth.

lines in the ionospheric it is frequently assumed that the parallel electric field is zero ($E_{||} = 0$). Since the field lines are then equipotentials and since the current flows mainly along the magnetic field lines, any static structures that exist should be essentially two dimensional, with the electric and magnetic fields perpendicular to the static magnetic field. If an east-west planar geometry is assumed, then the electric fields are associated with field-aligned charge sheets and the magnetic fields are associated with field-aligned currents sheets. If such two-dimensional static structures are present in the ionosphere, then one may question why the electric and magnetic fields would be so closely correlated. A convenient answer is provided by *Smiddy et al.* [1980]. If the field-aligned currents close in a meridian plane through the conducting layer at the base of the ionosphere, as illustrated in Figure 13, then the north-south electric field is related to the east-west magnetic field by the height-integrated Pedersen conductivity, Σ_P. It is relatively straightforward to show that $B/(\mu_0 E) = \Sigma_P$, where B is the east-west magnetic field and E is the north-south electric field. The correlation between the north-south electric field and the east-west magnetic field and the relation to the Pedersen conductivity have been previously noted and discussed by *Sugiura et al.* [1982].

It is easy to see in Figure 13 that the fluctuations in the north-south electric field and east-west magnetic field are correlated in such a way that the Poynting flux is directed downward, toward the earth, in agreement with the observations. The downward direction for the Poynting flux arises because energy is being dissipated by Joule heating at the base of the ionosphere. The origin of the energy required to drive this dissipation is not addressed by the basic model. The fact that the average Poynting flux is downward at altitudes up to several thousand kilometers indicates that the energy source must be located above this altitude range. Several possible energy sources can be identified. If the irregularities are produced by a shear-driven instability, as suggested by *Kintner* [1976] and *Kelley and Kintner* [1978], then the energy would come from the shear in the convective plasma flow. On the other hand, the spatial structure could also be related to a boundary condition imposed by electrostatic structures at high altitudes. *Mozer* [1981] has described electrostatic shocks at altitudes of several earth radii that might provide a suitable source. These electrostatic structures map to transverse scales lengths as small as 100 m in the ionosphere.

The static structure model can be tested by comparing the measured magnetic to electric field ratios with the Pedersen conductivity. Near the base of the ionosphere, $B/(\mu_0 E)$ should agree with the Pedersen conductivity. From the average values in Figure 10, and from the individual cases in Figures 7 and 8, it can be seen that the magnetic to electric field ratios measured at low altitudes correspond to a conductivity typically in the range of about 0.5–5 mhos. These conductivities are about an order of magnitude smaller than the conductivities of 8–20 mhos measured in diffuse auroras and discrete arcs by *Horwitz et al.* [1978] using radar backscatter techniques. Comparisons can also be made in specific cases by computing the Pedersen conductivity from the measured electron precipitation using the procedures of *Wallis and Budzinski* [1981] and *Spiro et al.* [1982]. For the spectrum in Figure 7 the Pedersen conductivity computed from the precipitated elec-

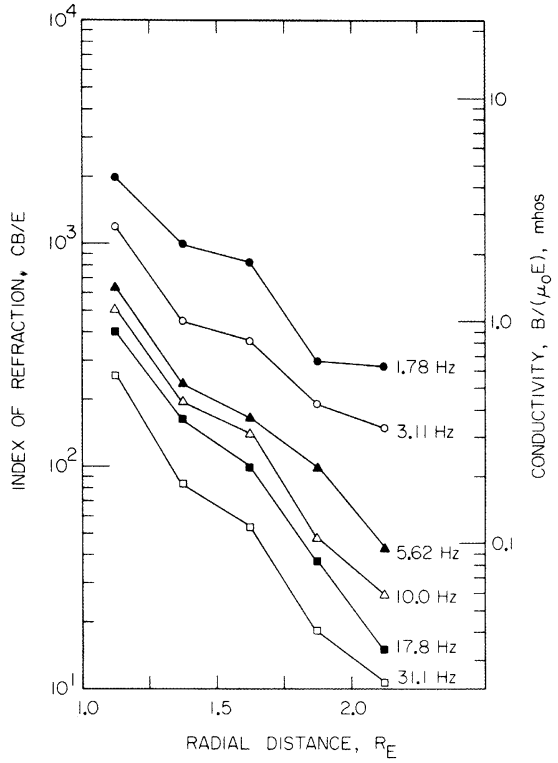

Fig. 10. A plot of the average magnetic to electric field ratio for all events studies expressed as a function of altitude. Note the strong tendency for the magnetic to electric field ratio to decrease with increasing radial distance and also with increasing frequency.

tron spectrum is $\Sigma_P = 4.7$ mhos. This value is about a factor of 5 higher than the conductivity determined from the magnetic to electric field ratio. These comparisons show that the measured $B/(\mu_0 E)$ ratios are usually significantly less than the accepted values for the height-integrated Pedersen conductivity. However, considering the uncertainties involved in computing the conductivity, these values may still be within an acceptable range. For example, for spatial scales less than a few hundred meters the current should start to close in the upper part of the conducting layer, thereby reducing the effective conductivity (C. Goertz, personal communication, 1983). Short-wavelength corrections of this type require further study.

A more sensitive test of the static structure model with $E_{\parallel} = 0$ is given by the radial dependence of the magnetic to electric field ratio. If it is assumed that the parallel electric field is zero and that the current responsible for the magnetic field is field aligned, then it is easy to show that the magnetic to electric field ratio is given by

$$\frac{B}{(\mu_0 E)} = \Sigma_P \left(\frac{1 + 3 \sin^2 \lambda_m}{1 + 3 \sin^2 \Lambda} \right)^{1/2} \tag{1}$$

where λ_m is the magnetic latitude and Λ is the invariant latitude. Near the earth, where $\lambda_m \simeq \Lambda$, the magnetic to electric field ratio is nearly independent of radial distance. This prediction is in strong disagreement with the observed radial dependence of $B/(\mu_0 E)$ in Figure 10, which shows that the magnetic to electric field ratio decreases rapidly with increasing radial distance. Thus the static structure model with $E_{\parallel} = 0$ is not able to account for an essential feature of the observations.

5.2. *Static Model ($E_{\parallel} \neq 0$)*

The only way that a purely static model could account for the observed radial dependence of the magnetic to electric field ratio is for a nonzero parallel electric field to be present. It is widely believed that parallel electric fields are present at high altitudes in the auroral zone. However, to determine the electric field mapping requires a detailed model for the parallel electric field. Simple conductivity models are unlikely to be satisfactory because the plasma is essentially collisionless at high altitudes. Most likely any parallel electric fields that exist are associated with double-layers [*Carlqvist*, 1972] or electrostatic shocks [*Mozer et al.*, 1977] and occur in regions with substantial field-aligned currents. Models for the electrostatic potential variation along the auroral field lines have been ana-

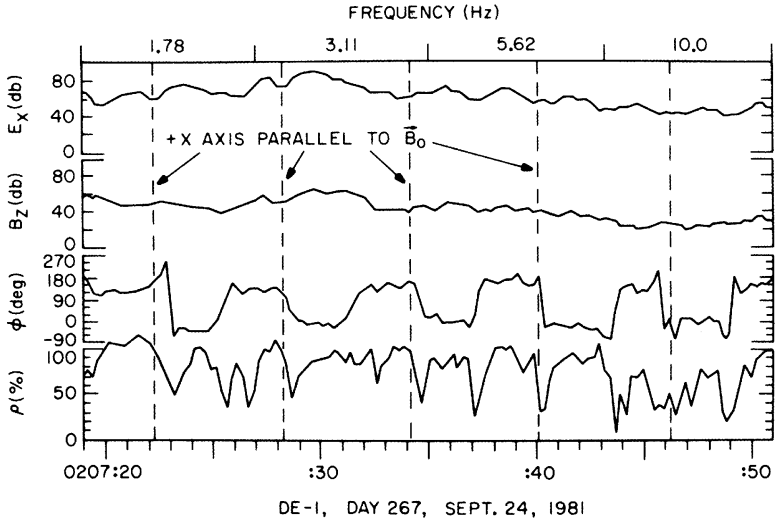

Fig. 11. A plot of the electric and magnetic field amplitudes, E_x and B_z, the relative phase ϕ, and correlation coefficient ρ, for a low-frequency noise event detected over the southern auroral zone. Note the relatively high correlation coefficient between the E_x and B_z fields and the square wave spin modulation pattern in the phase plot. These measurements show that the fluctuations in the E_x and B_z fields are closely correlated, with the Poynting flux directed downward toward the earth.

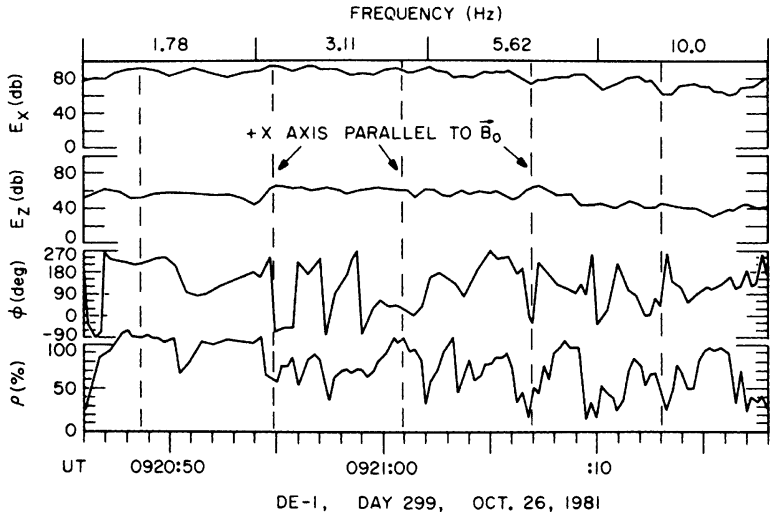

Fig. 12. A correlation plot similar to Figure 11 for the E_x and E_z fields. Although these fields have a relatively high correlation coefficient, often greater than 50%, the phase plot does not show a square wave spin modulation pattern, indicating that the perpendicular electric field is randomly polarized.

lyzed. For example, see *Chiu and Shulz* [1978] and *Lyons* [1980]. However, there models mainly deal with large-scale fields and do not consider small-scale irregualr fields. Because no suitable model exists for mapping the small-scale irregular fields, the validity of the static $E_{||} \neq 0$ model cannot be quantitatively tested at the present time.

Although a detailed model is not available for comparison with observations, certain qualitative features of the electric field mapping are known. If a perpendicular electric field is imposed at high altitudes, *Lyons* [1980] has shown that it is mainly the large-scale long-wavelength features that are mapped down to the conducting layer at the base of the ionosphere. These long-wavelength features would be coupled with magnetic field variations via the Pedersen conductivity, just as in the $E_{||} = 0$ static model. Short-wavelength features on the other hand tend to be screened out by polarization charges that develop along the auroral field lines. Qualitatively, this behavior is consistent with the observed radial variation of electric field intensities. As can be seen in Figure 9, the intensity of the low-frequency long-wavelength electric fields is nearly independent of altitude, whereas the intensity of the high-frequency short-wavelength fields decrease rapidly with decreasing altitude.

5.3. *Alfven Wave Model ($E_{||} = 0$)*

In the Alfven wave model the electric and magnetic field noise is attributed to electromagnetic waves propagating along the auroral field lines. This interpretation has the desirable feature of providing a ready explanation for the correlation between the electric and magnetic fields because the fluctuations are caused by an electromagnetic wave. At frequencies below the ion cyclotron frequency, the only known electromagnetic modes of propagation are the Alfven modes [*Stix*, 1962]. Two Alfven modes exist, called the fast and slow modes. Of these, only the slow (shear) mode has the proper polarization (**E** and **B** perpendicular to the static magnetic field) to explain the low-frequency noise. For this mode the component of the phase velocity along the static magnetic field, $\omega/k_{||}$, is the Alfven velocity, $V_A = B_0/(\mu_0\rho_m)^{1/2}$, where ρ_m is the mass density and B_0 is the static magnetic field. Normally, the Alfven velocity is much higher than the spacecraft velocity. Therefore as long as the wave normal is not too oblique to the magnetic field, the Doppler shift is negligible. The observed frequency is then the actual frequency of the wave. The case of highly oblique propagation is discussed in the next section.

The possibility of Alfven waves propagating along the auroral field lines has been suggested by several investigators, including, for example, *Scholer* [1970], *Goertz and Boswell* [1979], and *Lysak and Dum* [1983]. The basic idea is that if a disturbance is imposed on the auroral field lines at a large distance from the earth, this disturbance must be transmitted along the field line as an Alfven wave. It is easy to verify that for a source at several earth radii the round trip travel time for an Alfven wave through the ionosphere and back is several seconds. For typical convection speeds of a few kilometers per second, the plasma in the source will have moved several kilometers by the time the disturbance has propagated to the base of the ionosphere and back. Therefore for spatial scales

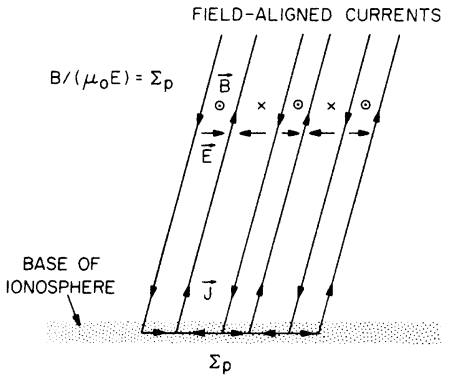

Fig. 13. An illustration showing how field-aligned currents closing through a conducting layer at the base of the ionosphere can produce closely correlated north-south electric and east-west magnetic fields. The magnetic to electric field ratio is determined by the height-integrated Pedersen conductivity, Σ_p.

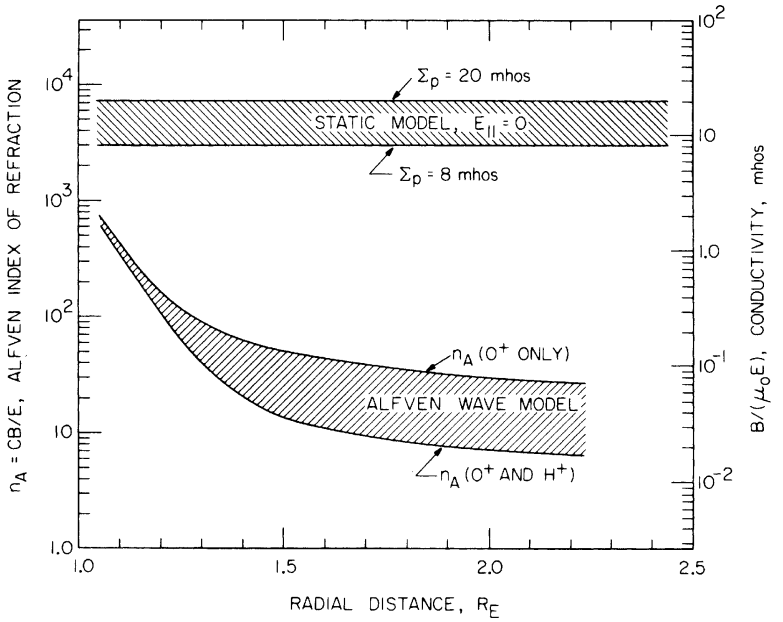

Fig. 14. A model of the Pedersen conductivity and the Alfven index of refraction as a function of radial distance for comparison with Figure 10. The electron density profile used in this model for n_A is taken from *Persoon et al.* [1983]. The upper limit on n_A assumes that the plasma is entirely O^+, and the lower limit assumes a transition from H^+ to O^+ at about 1.4 R_E. The limits on Σ_P are from *Horwitz et al.* [1978].

of a few kilometers or less, the propagation and reflection of Alfven waves between the magnetosphere and the base of the ionosphere is an essential feature of any dynamic model of ionosphere-magnetosphere coupling. This situation is somewhat analogous to the propagation of waves in a transmission line. The transient response of a transmission line consists of a series of reflected waves that bounce back and forth between the source and the termination. The magnetic to electric field ratio of the wave in the line alternates between the value determined by the termination and the value determined by the characteristic impedance of the transmission line.

The Alfven wave interpretation can be tested by comparing the magnetic to electric field ratio, cB/E, with the Pedersen conductivity, $\Sigma_P = B/(\mu_0 E)$, and the Alfven index of refraction, $n_A = c/V_A$. As in a transmission line, the observed magnetic to electric field ratio should lie between the value determined by the termination, $B/(\mu_0 E) = \Sigma_P$, and the characteristic impedance of the wave, $cB/E = n_A$. For Alfven waves propagating at all but very oblique angles to the earth's magnetic field, $cB/E = n_A$. The basic radial dependence of n_A is well established. Because of the exponential altitude variation of the O^+ plasma density, near the earth the Alfven index of refraction decreases exponentially with increasing altitude. At higher altitudes, beyond about 1.5 to 2.0 R_E, the index of refraction levels off and eventually starts to increase as the plasma composition changes from O^+ to H^+. To conduct a quantitative comparison, a specific plasma density model is needed. Near the earth, at altitudes below a few thousand kilometers, the plasma density has been extensively studied by low-altitude polar-orbiting spacecraft. For example, see *Chan and Colin* [1969] or *Brace* [1970]. Farther from the earth, fewer measurements are available and the density profile is less well known. Recently, a study of the electron density profile over the polar region has been carried out by *Persoon et al.* [1983], using data from DE 1. Although this study was restricted to the polar cap, comparisons in specific cases show that the density in the auroral regions is usually only slightly lower than the polar cap densities. Using the density profile obtained by *Persoon et al.* [1983] at high altitudes and the densities measured by *Chan and Colin* [1969] at low altitudes, the model shown in Figure 14 has been constructed. The shaded region marked "Alfven wave model" indicates the estimated range of n_A values. The wide range of uncertainty at high altitudes is due to the unknown plasma composition and scale height at high altitudes. The upper limit assumes that the plasma is entirely O^+, and the lower limit assumes a transition form O^+ to H^+ at about 1.4 R_E. Because this is an "average" model, significant deviations can be expected because of seasonal effects, auroral activity, and other factors, particularly at high altitudes.

Comparing the measured cB/E ratios in Figure 10 with the model for the radial variation of the Alfven index of refraction in Figure 14, it can be seen that both cB/E and n_A decrease rapidly with increasing radial distance. Usually, the measured cB/E ratios lie somewhat above n_A. This tendency can be verified in specific cases. For example, in Figure 7 a typical auroral electron density at $R = 1.22$ R_E is $n_e \simeq 10^3$ cm^{-3} [*Chan and Colin*, 1969], which gives $n_A = 54$. The top panel of Figure 7 shows that the measured cB/E ratios are about a factor of 10 larger than the n_A values given by the model. Similarly, in Figure 8 a typical auroral electron density at $R = 1.10$ R_E is $n_e \simeq 10^5$ cm^{-3} [*Chan and Colin*, 1969], which gives $n_A = 325$. The measured cB/E ratios in this case are about a factor of 5 larger than the n_A values given by the model. Typically, the magnetic to electric field ratio is about a factor of 2 to 10 above the value determined by the Alfven index of refraction but always well below the value determined by the Pedersen conductivity. This result is consistent with the expectation of an Alfven wave model. As discussed by *Goertz and Boswell* [1979] and others, the magnetic to electric field

ratio is determined by a superposition of the incident and reflected waves and must lie between the values determined by the termination at the end of the field line, $B/(\mu_0 E) = \Sigma_P$, and the characteristic impedance of the Alfven wave, $cB/E = n_A$.

Although the cB/E ratios are consistent with the Alfven wave model, there are several difficulties that remain to be explained. One of these is the frequency dependence of the index of refraction. As can be seen in Figure 10, the index of refraction tends to decrease with increasing frequency. For frequencies below the O^+ cyclotron frequency, the Alfven index of refraction should be essentially independent of frequency. Although a serious difficulty, this disagreement does not completely rule out an Alfven wave interpretation. The observed electric to magnetic field ratio involves a superposition of an incident and a reflected wave. If the reflection coefficient depends on frequency, as it almost certainly does, then the electric to magnetic field ratio will depend on frequency. For an Alfven wave propagating through a conducting layer it is easy to show that the lowest frequencies have the least asborption and therefore the highest reflection coefficient. Since a higher reflection coefficient tends to decrease the electric field strength, the magnetic to electric field strength would be expected to increase at lower frequencies. Although this explanation appears to give the proper frequency dependence, further quantitative analysis is needed to evaluate the reflection coefficient for a realistic model of the conducting layer. Another possible explanation for the frequency dependence of cB/E is also given below.

5.4. *Kinetic Alfven Wave Model ($E_{\|} \neq 0$)*

If the wave normal angle of the shear Alfven mode is sufficiently large, then the wave can develop an electric field component parallel to the magnetic field. In this regime the wave is called a kinetic Alfven wave. Kinetic Alfven waves were first discussed by *Hasegawa* [1977]. Because of their parallel electric field, kinetic Alfven waves have been considered as a method of accelerating particles along the auroral field lines [*Goertz and Boswell*, 1979; *Lysak and Dum*, 1983]. The basic scale length of importance for a kinetic Alfven wave is the ion cyclotron radius. As the angle between the wave normal and the static magnetic field approaches perpendicular, the transverse wavelength approaches the ion cyclotron radius. In this regime the wave becomes electrostatic with $E_{\|} \neq 0$.

For typical temperatures in the auroral ionosphere ($T \simeq 10^4$ °K) at low altitudes ($R \simeq 1.2\ R_E$) the cyclotron radius is only about 20 m for O^+ ions and 5 m for H^+ ions. If the low-frequency electric and magnetic noise detected by DE 1 is due to kinetic Alfven waves, then the wavelength of these waves could be very short, possibly only a few tens of meters. For such short wavelengths the Doppler shift is considerable, in some cases much larger than the rest frame frequency. The observed frequency spectrum would then be determined mainly by the transverse wave number. The short wavelength of kinetic Alfven waves could possibly explain why the cB/E ratio tends to decrease with increasing frequency. For highly oblique propagation the higher frequencies would be mainly due to very short wavelength waves. These waves would be expected to have a lower cB/E ratio because of their large electrostatic component [see *Hasegawa*, 1977]. The kinetic Alfven wave model has the further merit of explaining why the noise sometimes appears to have a cutoff near the O^+ cyclotron frequency. As is well known [*Stix*, 1962], the shear Alfven wave has an upper frequency cutoff at the ion cyclotron frequency. For waves that are not too oblique the Doppler shift would be small and a cutoff effect would be observed near f_{cO+}. On the other hand, if highly oblique waves are also present, then the Doppler shift would tend to spread the frequency spectrum above f_{cO+}, thereby obscuring the cutoff.

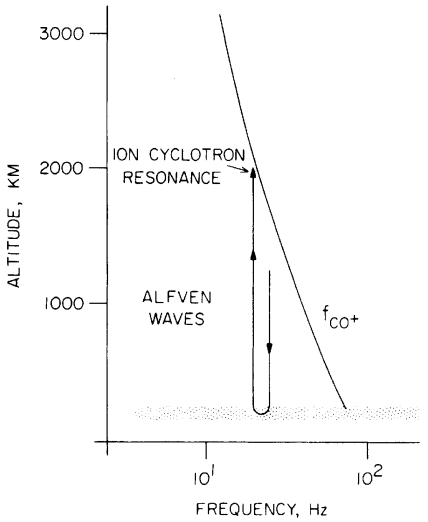

Fig. 15. A plot of the O^+ cyclotron frequency as a function of altitude showing how a shear Alfven reflected from the ionosphere would be absorbed by ion cyclotron damping at the O^+ cyclotron frequency. This absorption could heat O^+ ions, possibly producing ion conics and other nonthermal ion distributions.

The possibility that the low-frequency noise may consist of Alfven waves may have some interesting implications for ion heating in the auroral regions. Although the average energy flow is directed toward the earth, a substantial amount of the wave energy should be reflected from the ionosphere, is illustrated in Figure 15. As the reflected waves propagate upward, the left-hand-polarized component will be absorbed by ion cyclotron damping at the O^+ cyclotron frequency. Because the wave energy integrated over the auroral zones (2×10^{-2} erg cm^{-2}, over an area of 2×500 km $\times$ 6000 km) is very large, approximately 1.2×10^8 W, the energy input into the O^+ ions could be appreciable. This heating could possibly account for the upflowing O^+ conics reported by H. L. Collins et al. (unpublished manuscript, 1984) and *Yau et al.* [1984]. Rough estimates by A. W. Yau (personal communication, 1983) indicate that a total power of about 5×10^7 W is required to account for the outflowing O^+ ions observed during quiet times, increasing to about 1.6×10^8 W during disturbed times. The possibility of resonant absorption of left-hand-polarized ion cyclotron waves as a mechanism for heating ions is not new. Ion cyclotron waves have been used for ion heating in laboratory plasmas, and *Temerin and Lysak* [1984] have already suggested that H^+ electromagnetic ion cyclotron waves could be responsible for producing H^+ ion conics.

6. CONCLUSION

We have described the DE-1 measurements of intense low-frequency electric and magnetic noise observed at low altitudes over the auroral zone. The intensity of both the electric and magnetic fields decreases rapidly with increasing frequency. Most of the energy is at frequencies below the O^+ cyclotron frequency, and in some cases evidence for a cutoff or change in spectral slope can be seen near f_{cO+}. The magnetic

to electric field ratio decreases rapidly with increasing radial distance and also decreases with increasing frequency. The polarization of the electric field in a plane perpendicular to the earth's magnetic field is essentially random. Phase measurements show that the transverse electric and magnetic fields are closely correlated, with the average Poynting flux directed downward, toward the earth. The total electromagnetic power flow associated with the noise is substantial, approximately 10^8 W integrated over both auroral zones. The source of this noise must be located along the auroral field lines at altitudes of several thousand kilometers or more.

Two general models were discussed to interpret these observations, one based on static electric and magnetic fields imbedded in the ionosphere and the other based on Alfven waves propagating along the auroral field lines. For the static model the magnetic to electric field ratio at the base of the ionosphere is determined by the height-integrated Pedersen conductivity, $B/(\mu_0 E) = \Sigma_P$. The frequency spectrum would then be determined by the Doppler shift as the spacecraft moves through the irregular field structures. If the parallel electric field is assumed to be zero ($E_{||} = 0$), the electric and magnetic field structure is essentially two dimensional, and the magnetic to electric field ratio, $B/(\mu_0 E)$, is nearly independent of radial distance. The static model with $E_{||} = 0$ disagrees strongly with the observations, since cB/E is observed to decrease rapidly with increasing radial distance. The only way that a static model can be brought into agreement with the observations is for a nonzero parallel electric field ($E_{||} \neq 0$) to be present along the auroral field lines. Although a nonzero parallel electric field is plausible, at the present time no suitable theory exists to predict the radial dependence of the electric field. Therefore no firm conclusions can be drawn about the validity of the static model with $E_{||} \neq 0$.

Two types of Alfven wave models were considered, one for wave normal angles not too oblique to the magnetic field and the other for wave normal angles nearly perpendicular to the magnetic field. For the nonoblique case the parallel electric field is essentially zero ($E_{||} = 0$). For these waves the Doppler shift is essentially negligible, so the observed spectrum is the actual frequency spectrum of the waves. The observed radial variation of cB/E, decreasing rapidly with increasing radial distance, is in reasonable agreement with the Alfven wave model. The magnetic to electric field ratio always lies between the values determined by the Alfven index of refraction, $cB/E = n_A$, and the Pedersen conductivity, $\Sigma_P = B(\mu_0 E)$. Although the radial variation of cB/E is consistent with an Alfven wave model, the cB/E ratio tends to decrease with increasing frequency, contrary to the expected frequency dependence of the Alfven index of refraction. This disagreement could possibly be accounted for by a frequency dependent reflection of waves from the base of the ionosphere. For wave normal angles nearly perpendicular to the magnetic field, finite ion cyclotron radius effects can be important. Under these conditions the perpendicular wavelength of the wave can become very short, the parallel electric field is no longer zero ($E_{||} \neq 0$), and the wave becomes increasingly electrostatic. These waves are called kinetic Alfven waves. For kinetic Alfven waves the Doppler shift is very large if the perpendicular wavelengths are near the ion cyclotron radius. The existence of such short-wavelength Alfven waves could possibly explain the frequency dependence of the cB/E ratio as well as the tendency for a diffuse cutoff to occur near the O^+ cyclotron frequency.

At the present time we are not able to definitely conclude which, if any, of the above models is able to explain the correlated electric and magnetic field noise observed by DE 1. The only firm conclusion that can be made is that the static model with $E_{||} = 0$ is not a viable alternative because it does not predict the observed radial variation of $B/(\mu_0 E)$. Unfortunately, the basic mechanism responsible for the noise is also not known. The irregularities or waves could be produced by a shear-driven MHD turbulence process, such as suggested by *Kintner* [1976], or by a kinetic instability driven by free energy in the auroral electron or ion distributions. Whatever the type of irregularities or mode of propagation, it is known that the source is located at relatively high altitudes, since the average energy flow is always toward the earth, even at radial distances up to 2 R_E. The total power involved is substantial, at least 10^8 W. Most of this energy is probably dissipated in the conductive layer at the base of the ionosphere. However, if the noise is caused by Alfven waves and if some of the energy is reflected from the base of the ionosphere, then the reflected waves could possibly play a role in ion acceleration if they are absorbed at the ion cyclotron frequency.

Acknowledgments. The authors would like to acknowledge useful discussions of the interpretation of these data with L. Brace and N. Maynard of NASA Goddard Space Flight Center and with C. Goertz at the University of Iowa. The authors also express their thanks to the two referees who provided many useful comments and suggestions. The research at the University of Iowa was supported by NASA through grant NAG5-310 from Goddard Space Flight Center, grants NGL-16-001-002 and NGL-16-001-043 from NASA Headquarters, and by the Office of Naval Research through grant N00014-76-C-0016. The research at Southwest Research Institute was supported by NASA through contracts NAS5-26363 and NAS5-25693 from Goddard Space Flight Center and Air Force Geophysics Laboratory through contract AFGL 712183N0001.

The Editor thanks P. M. Kintner and M. Temerin for their assistance in evaluating this paper.

REFERENCES

Akasofu, S.-I., Dynamic morphology of auroras, *Space Sci. Rev.*, *4*, 498, 1965.

Brace, L. H., The global structure of ionospheric temperature, *Space Res.*, *X*, 633, 1970.

Burch, J. L., J. D. Winningham, V. A. Blevins, N. Eaker, and W. C. Gibson, High-altitude plasma instrument for Dynamics Explorer-A, *Space Sci. Instrum.*, *5*, 455, 1981.

Carlqvist, P., On the formation of double layers in plasmas, *Cosmic Electrodyn.*, *3*, 377, 1972.

Chan, K. L., and L. Colin, Global electron density distributions from topside soundings, *Proc. IEEE*, *57*, 990, 1969.

Chiu, Y. T., and M. Schulz, Self-consistent particle and parallel electric field distributions in the magnetosphere-ionosphere auroral regions, *J. Geophys. Res.*, *83*, 629, 1978.

Curtis, S. A., W. R. Hoegy, L. H. Brace, N. C. Maynard, and M. Sugiura, DE-2 cusp observations: Role of plasma instabilities in topside ionospheric heating and density fluctuations, *Geophys. Res. Lett.*, *9*, 997, 1982.

Goertz, C. K., and R. W. Boswell, Magnetosphere-ionosphere coupling, *J. Geophys. Res.*, *84*, 7239, 1979.

Gurnett, D. A., and L. A. Frank, ELF noise bands associated wth auroral electron precipitation, *J. Geophys. Res.*, *77*, 3411, 1972.

Gurnett, D. A., and L. A. Frank, A region of intense plasma wave turbulence on auroral field lines, *J. Geophys. Res.*, *82*, 1031, 1977.

Hasegawa, A., Kinetic properties of Alfven waves, *Proc. Indian Acad. Sci.*, *86*, 151, 1977.

Heppner, J. P., Magnetospheric convection patterns inferred from high latitude activity, in *Atmospheric Emissions*, edited by B. M. McCormac and A. Omholt, p. 251, Reinhold, New York, 1969.

Horwitz, J. L., J. R. Doupnik, and P. M. Banks, Chatanika radar observations of the latitudinal distributions of auroral zone electric fields, conductivities, and currents, *J. Geophys. Res.*, *83*, 1463, 1978.

Kelley, M. C., and P. Kintner, Two-dimensional turbulence in a low β cosmic scale plasma, *Astrophys. J.*, *220*, 339, 1978.

Kelley, M. C., and F. S. Mozer, A satellite survey of vector electric

fields in the ionosphere at frequencies of 10 to 500 Hz, 1, Isotropic, high-altitude electrostatic emissions, *J. Geophys. Res.*, *77*, 4158, 1972.

Kintner, P. M., Jr., Observations of velocity shear driven plasma turbulence, *J. Geophys. Res.*, *81*, 5114, 1976.

Lyons, L. R., Generation of large-scale regions of auroral currents, electric potentials, and precipitation by the divergence of the convection electric field, *J. Geophys. Res.*, *85*, 17, 1980.

Lysak, R. L., and C. T. Dum, Dynamics of magnetosphere-ionosphere coupling including turbulent transport, *J. Geophys. Res.*, *88*, 365, 1983.

Maynard, N. C., and J. P. Heppner, Variations in electric fields from polar orbiting satellites, in *Particles and Fields in the Magnetosphere*, edited by B. M. McCormac, p. 247, Reinhold, New York, 1970.

Maynard, N. C., J. P. Heppner, and A. Egeland, Intense, variable electric fields at ionospheric altitudes in the high latitude regions as observed by DE-2, *Geophys. Res. Lett.*, *9*, 981, 1982.

Mozer, F. S., ISEE 1 observations of electrostatic shocks on auroral field lines between 2.5 and 7 earth radii, *Geophys. Res. Lett.*, *8*, 823, 1981.

Mozer, F. S., C. W. Carlson, M. K. Hudson, R. B. Torbett, B. Parady, J. Yatteau, and M. C. Kelley, Observations of paired electrostatic shocks in the polar magnetosphere, *Phys. Rev. Lett.*, *38*, 292, 1977.

Persoon, A. M., D. A. Gurnett, and S. D. Shawhan, Polar cap electron densities from DE 1 plasma wave observations, *J. Geophys. Res.*, *88*, 10,123, 1983.

Potemra, T. A., Birkeland currents: Present understanding and some remaining questions, in *High-Latitude Space Plasma Physics*, edited by B. Hultqvist and T. Hagfors, p. 335, Plenum, New York, 1983.

Scholer, M., On the motion of artificial ion clouds in the ionosphere, *Planet. Space Sci.*, *18*, 977, 1970.

Shawhan, S. D., D. A. Gurnett, D. L. Odem, R. A. Helliwell, and C. G. Park, The plasma wave and quasi-static electric field instrument (PWI) for Dynamics Explorer-A, *Space Sci. Instrum.*, *5*, 535, 1981.

Smiddy, M., W. J. Burke, M. C. Kelley, N. A. Saflekos, M. S. Gussenhoven, D. A. Hardy, and F. J. Rich, Effects of high-latitude conductivity on observed convection electric fields and Birkeland currents, *J. Geophys. Res.*, *85*, 6811, 1980.

Spiro, R. W., P. H. Reiff, and L. J. Maher, Jr., Precipitating electron energy flux and auroral zone conductances—An empirical model, *J. Geophys. Res.*, *87*, 8215, 1982.

Stix, T. H., *The Theory of Plasma Waves*, McGraw-Hill, New York, 1962.

Sugiura, M., N. C. Maynard, W. H. Farthing, J. P. Heppner, B. G. Ledley, and L. J. Cahill, Jr., Initial results on the correlation between the magnetic and electric fields observed from the DE-2 satellite in the field-aligned current regions, *Geophys. Res. Lett.*, *9*, 985, 1982.

Temerin, M., The polarization, frequency, and wavelength of high-latitude turbulence, *J. Geophys. Res.*, *83*, 2609, 1978.

Temerin, M., and R. L. Lysak, Electromagnetic ion cyclotron (ELF) waves generated by auroral electron precipitation, *J. Geophys. Res.*, *89*, 2849, 1984.

Wallis, D. D., and E. E. Budzinski, Empirical models of height-integrated conductivities, *J. Geophys. Res.*, *86*, 125, 1981.

Yau, A. W., B. A. Whalen, W. K. Peterson, and E. G. Shelley, Distribution of upflowing ionospheric ions in the high-altitude polar cap and auroral ionosphere, *J. Geophys. Res.*, *89*, 5507, 1984.

Zmuda, A. J., and J. C. Armstrong, The diurnal variation of the region with vector magnetic field changes associated with field-aligned currents, *J. Geophys. Res.*, *79*, 2501, 1974*a*.

Zmuda, A. J., and J. C. Armstrong, The diurnal flow pattern of field-aligned currents, *J. Geophys. Res.*, *79*, 4611, 1974*b*.

J. L. Burch, J. D. Menietti, and J. D. Winningham, Southwest Research Institute, P. O. Drawer 28510, San Antonio, TX 78284.

D. A. Gurnett and R. L. Huff, Department of Physics and Astronomy, University of Iowa, Iowa City, IA 52242.

S. D. Shawhan, NASA Headquarters, 400 Maryland Avenue, Washington, D. C. 20546.

(Received February 23, 1984;
revised May 8, 1984;
accepted May 29, 1984.)